

## ARTICLE

# Numerical Study of Vibrational Energy Relaxation of O–H Bending in Liquid H<sub>2</sub>O

Guo-cai Tian\*

*State Key Laboratory of Molecular Reaction Dynamics, Institute of Chemistry, Chinese Academy of Sciences, Beijing 100080, China; Faculty of Materials and Metallurgical Engineering, Kunming University of Science and Technology, Kunming 650093, China*

(Dated: Received on January 3, 2007; Accepted on February 4, 2007)

The relaxation of O–H bending of water molecule H<sub>2</sub>O in the liquid phase was studied with the molecular dynamics simulation approach. Both rigid and flexible solvents were used to identify the different channels for the vibrational energy relaxation. It was observed that the relaxation time for the O–H bend overtone is 174 fs in the rigid solvent while it is 115 fs in the flexible solvent. The main pathway of the O–H bend overtone is transition to the bend fundamental. The relaxation time of the O–H bend fundamental was calculated as 204 fs which is comparable to the experimental value 170 fs.

**Key words:** Vibrational energy relaxation, O–H bending, Liquid water, Landau-Teller theory, Molecular dynamics simulation

## I. INTRODUCTION

In condensed phases a vibrational mode normally interacts with many other modes. As this mode is excited, it will dissipate its energy to the surrounding degrees of freedom. This process is called vibrational energy relaxation (VER), a fundamental process in chemistry, physics and biology [1-3]. The study of VER provides the details of the interactions between a molecule and other involved molecules. Knowing the interactions is crucial to understanding many important physical chemical properties, such as chemical reactivity and solvation dynamics as well as transport features [4,5]. With recent advances in laser and time resolved pump-probe technology, the ultrafast spectroscopic methods are powerful tools to probe both intramolecular vibrational energy redistribution and intermolecular vibrational energy relaxation on picoseconds or faster time scales in condensed phases [1-12]. However, experimental measurements give only the vibrational energy relaxation time; it is difficult to obtain the molecular mechanism of VER directly [12]. Over the last decades, a number of theoretical methods such as Landau-Teller theory [8-11], the quantum path integral molecular dynamics method [12], mixed quantum-classical approaches [13], the instantaneous pair theory [14], and centroid molecular dynamics [15] have been proposed and successfully used to reveal the molecular mechanism of the VER for various systems such as CH<sub>3</sub>Cl in H<sub>2</sub>O [16], HOD in D<sub>2</sub>O [17-19], CN<sup>-</sup> in H<sub>2</sub>O [20], N<sub>3</sub><sup>-</sup> in H<sub>2</sub>O [21], and neat methanol [22].

Because most chemical and biochemical reactions occur in aqueous solution, it is necessary to elucidate the structural and dynamical properties of liquid water itself in order to fully understand the mechanism of those reactions. In recent years the vibrational dynamics of O–H/O–D stretching of HOD in diluted liquid D<sub>2</sub>O or H<sub>2</sub>O have been extensively tested by using ultrafast experiments [2,23-27], and many useful results have been obtained. Theoretically, Rey and Hynes (RH) [2,17] and Lawrence and Skinner (LS) [18,19] have done a series of studies to analyze the vibrational energy relaxation mechanism of HOD in liquid D<sub>2</sub>O. Very recently the author [28] has been able to explain the relaxation mechanism for O–D stretching of HOD in diluted H<sub>2</sub>O. All these theoretical or numerical investigations are based on the Landau-Teller type theory. Since many experimental and theoretical efforts are performed on the OH/OD stretching of HOD in D<sub>2</sub>O or H<sub>2</sub>O, an important question is how the dynamics of liquid water itself behaves. Recently, experimental studies on the vibrational dynamics in pure liquid water have been performed by Dlott [29-31], Elessaer [32-34], Lindner [35], and Wouterson [36]. But the microscopic mechanism is still not fully understood and different relaxation mechanisms have been proposed. For example, Dlott concluded that at least one of the two pathways, O–H stretch to bend overtone or O–H stretch to two bend fundamentals, is probably in competition with the O–H stretch to bend fundamental [29-31], while a transfer of energy to the O–H bend fundamental is provided by other groups [33-36]. Because the O–H bending vibrational mode is the intramolecular mode with the lowest frequency, it represents a crucial gateway for dissipating the intramolecular energy. It is thus important to elucidate the molecular mechanism of O–H bend relaxation to understand the intra- and intermolecular vibrational

\*Author to whom correspondence should be addressed. E-mail: tiangc@iccas.ac.cn, Fax: +86-10-62563167. Also at the Graduate School, Chinese Academy of Sciences, Beijing, China

relaxation of pure liquid water.

Recent femtosecond infrared pump-probe studies of a H<sub>2</sub>O:HOD:D<sub>2</sub>O mixture gave an O–H bending lifetime of 400 fs [36]. In contrast, a substantially longer lifetime of 1.4 ps has been derived [31]. Most recently, Lindner reported a lifetime of 260 fs for O–H bending in pure liquid water [35] while a lifetime of 170 fs is provided by Elsaesser [34]. However, the relaxation mechanism is not clear and no theoretical investigation of the problem has been reported. In this paper, Landau-Teller theory and molecular dynamics simulations are employed to reveal the molecular mechanism of O–H bending relaxation in pure water. The results offer an explanation for available experimental findings and make predictions for the experimental verifications.

## II. SYSTEMS AND METHODS

The system considered in present work is a single, tagged H<sub>2</sub>O in a bath of 499 solvent H<sub>2</sub>O molecules. Both rigid and flexible solvents are considered to clarify the different channels for the vibrational energy relaxation. The potential energy functions and the methodology applied are as follows.

### A. Potential energy surface

To facilitate the simulation speed, the potential energy surface proposed by Sceats and Rice [37] was used to describe the vibrational modes of the tagged H<sub>2</sub>O molecule whereas the SPC/E model [38] was used to define the intermolecular potential of the rigid solvent H<sub>2</sub>O molecules. For flexible solvent H<sub>2</sub>O molecules, by contrast, the intramolecular potential is given by [39-41]

$$V = D_0\{[1 - \exp(-\beta\Delta r_1)]^2 + [1 - \exp(-\beta\Delta r_2)]^2\} + \frac{k_\alpha}{2}r_e^2\Delta\alpha^2 + k_{r\alpha}r_e\Delta\alpha(\Delta r_1 + \Delta r_2) + k_{r,r'}(\Delta r_1\Delta r_2) \quad (1)$$

where  $\Delta r_1$  and  $\Delta r_2$  denote the displacements of the two O–H bond lengths from the equilibrium value  $r_e$ , and  $\Delta\alpha$  is the change of the H–O–H angle. Parameters used in Eq.(1) are listed in Table I. The solvent-solute as well as solute-solvent intermolecular interactions are simply a pairwise sum of Lennard-Jones (L-J) and Coulomb terms, namely,

$$V^{\text{inter}} = \sum_{i<j} \left\{ 4\varepsilon_{ij} \left[ \left( \frac{\sigma_{ij}}{r_{ij}} \right)^{12} - \left( \frac{\sigma_{ij}}{r_{ij}} \right)^6 \right] + \frac{1}{4\pi\varepsilon_0} \frac{q_i q_j}{r_{ij}} \right\} \quad (2)$$

where  $\varepsilon$  and  $\sigma$  are the L-J parameters and  $r_{ij}$  denotes the distance between the L-J sites  $i$  and  $j$ ,  $q_i$  and  $q_j$  are

TABLE I Intramolecular potential for flexible solvent H<sub>2</sub>O

|                                       |         |
|---------------------------------------|---------|
| $D_0/(\text{mdyn}/\text{\AA})$        | 0.640   |
| $\beta/(\text{\AA}^{-1})$             | 2.567   |
| $k_\alpha(\text{mdyn}/\text{\AA})$    | 0.7610  |
| $k_{r\alpha}(\text{mdyn}/\text{\AA})$ | 0.2280  |
| $k_{r,r'}/(\text{mdyn}/\text{\AA})$   | -0.1010 |
| $r_{1e}/\text{\AA}$                   | 1.0     |
| $r_{2e}/\text{\AA}$                   | 1.0     |
| $\alpha_e$                            | 109.47  |

the point charges on site  $i$  and  $j$ . The L-J parameters and point charges are taken from the original SPC/E model [38].

### B. Methodology

The Landau-Teller theory, which has been widely and successfully applied to study the VER in condensed phases [2,9-11,17-19], is used to reveal the VER of the O–H bending for the H<sub>2</sub>O molecule in liquid water. The theory is based on the perturbation treatment. For a condensed-phase system the Hamiltonian consists of three parts, that is,

$$H = H_s + H_b + V \quad (3)$$

where  $H_s$  is the system Hamiltonian describing the quantum mechanical vibration of the tagged water molecule;  $H_b$  represents the bath Hamiltonian which includes all of degrees of freedom of solvent molecules and the translational, rotational degrees of freedom of the tagged water molecule; and  $V$  is the interaction between the system and the bath.

The rate constant  $k_{if}$  of the energy transfer between the vibrational states  $i$  and  $f$  can be obtained from Fermi's golden rule,

$$k_{if} = \frac{1}{\hbar^2} \int_{-\infty}^{+\infty} dt \exp(i\omega_{if}t) \langle V_{if}(t) V_{fi}(0) \rangle_b \quad (4)$$

where  $\omega_{if} = (E_i - E_f)/\hbar$  is the transition frequency,  $V_{if}(t) = e^{iH_b t/\hbar} \langle i|V|f \rangle e^{-iH_b t/\hbar}$  is the coupling between the system and the bath in the interaction representation with respect to the bath, and  $\langle V_{if}(t) V_{fi}(0) \rangle_b = \text{Tr}_b[e^{-H_b/kT} V_{if}(t) V_{fi}]/\text{Tr}_b(e^{-H_b/kT})$  is nothing but the quantum mechanical interaction time correlation function (TCF).

To calculate the vibrational energy transfer rate constant via Eq.(4), the interaction Hamiltonian  $V$  is usually expanded in the Taylor series with respect to the normal mode coordinate of the solute, namely,

$$V = \sum_{\alpha} F_1^{\alpha}(t) q_{\alpha} + \frac{1}{2} \sum_{\alpha, \beta} F_2^{\alpha, \beta}(t) q_{\alpha} q_{\beta} + \dots \quad (5)$$

where  $F_1^\alpha(t) = -\partial V/\partial q_\alpha$  and  $F_2^{\alpha,\beta}(t) = -\partial^2 V/\partial q_\alpha \partial q_\beta$  are the forces on the normal mode and the Hessian matrices respectively. If the terms with orders higher than the first are neglected, one obtains [9,11]

$$k_{if} = \frac{1}{\hbar^2} \sum_{\alpha} \langle i | q_{\alpha} | f \rangle^2 \cdot \int_{-\infty}^{\infty} dt e^{i\omega_{if}t} \langle F_1^\alpha(t) F_1^\alpha(0) \rangle_b \quad (6)$$

where  $\langle i | q_{\alpha} | f \rangle$  is the transition matrix element.

It is obvious that the key quantity needed to calculate in Eq.(6) is the force-force TCF  $\langle F_1^\alpha(t) F_1^\alpha(0) \rangle_b$ . But this quantity is difficult to determine from a direct quantum mechanical calculation for many-body systems, because the computational effort increases exponentially with the number of degrees of freedom. Therefore, one has to apply some approximations [2,9,42,43] for real systems. The common approach is to treat the bath classically and finally multiply a quantum correction factor (QCF)  $Q(\omega)$  to the rate constants [2,9,11,17-19], namely,

$$k_{if} = \frac{Q(\omega_{if})}{\hbar^2} \sum_{\alpha} \langle i | q_{\alpha} | f \rangle^2 \cdot \int_{-\infty}^{\infty} dt e^{i\omega_{if}t} \langle F_1^\alpha(t) F_1^\alpha(0) \rangle_b^{cl} \quad (7)$$

Now one needs to compute the classical TCF of the forces exerted on the solute normal mode of the tagged water molecule. This quantity can be calculated from the classical molecular dynamics simulation at each time step with some mathematical manipulation [44].

A number of QCFs are suggested in Refs.[45-47], but for a specific problem, there is not a general rule to choose the QCF. In this work, The authors use the same method as the previous work [28] in which we chose the QCF based on the mechanism of the relaxation process (see Refs.[18,19,28,47] for the details). A transition between the two vibrational states of H<sub>2</sub>O with or without solvent vibrations can lead to two kinds of relaxation mechanism. For the transition without solvent vibrations, only several quanta of bath translations and rotations are excited or depleted, which is similar to the case of multiphonon relaxation in solids. We use the Harmonic/Schofield QCF that works well for multiphonon like process [18,47], namely,

$$Q(\omega) = e^{\beta\hbar\omega/4} \left( \frac{\beta\hbar\omega}{1 - e^{-\beta\hbar\omega}} \right)^{1/2} \quad (8)$$

For the transition between two states with solvent vibrations and  $\omega_{if} > 0$ , which involves the excitation one quantum solvent vibration at solvent frequency  $\omega_s$  (a form of intermolecular vibration-vibration transfer) as well as the creation or depletion of one or more quanta of bath transitions and rotations to conserve energy when

the vibrational mode of solute is not exactly resonant with the vibration of solvent molecule, the QCF  $Q_V(\omega)$  is [45]

$$Q_V(\omega) = Q_H(\omega_s) Q_{HS}(\omega - \omega_s) \quad (9)$$

where  $Q_H(\omega)$  is Harmonic QCF given by [18,19,47]

$$Q_H(\omega) = \frac{\beta\hbar\omega}{1 - \exp(-\beta\hbar\omega)} \quad (10)$$

The rate constant can be written as a sum of the classical rate constants of these two pathways with appropriate QCF, namely, where  $k_{if}^R$  and  $k_{if}^V$  are the classical rate without solvent vibration and vibration-vibration transfer respectively. These quantities can be obtained as follows. One performs a simulation with rigid solvent molecules and calculates the classical TCF and its Fourier transform to get  $k_{if}^R$ . Another simulation with flexible solvent molecules, which includes all mechanisms is performed to obtain the total classical rate constant  $k_{if}^T$ . Then we can find  $k_{if}^V = k_{if}^T - k_{if}^R$ .

### C. Computer simulation details

Two separate simulations were performed with rigid and flexible H<sub>2</sub>O molecules in *NVE* (constant number of particles, volume and energy) ensemble by the molecular dynamics simulation package DL-POLY 2.14 program [48]. Cubic periodic boundary conditions were used, where the size of the simulation box was chosen to yield an experimental density for H<sub>2</sub>O at 300 K. The electrostatic forces were treated using the Ewald summation procedure and the internal geometry of the tagged H<sub>2</sub>O was kept via the SHAKE algorithm [49]. The simulation trajectory was propagated by the leapfrog algorithm with a time step of 0.5 fs. Each system was equilibrated at 300 K by periodically rescaling the velocities of the molecules until the temperature was kept within  $\pm 2$  K for 80 ps without further adjustment, after which a production run of 2 ns was performed to calculate the quantities of interest.

## III. RESULTS AND DISCUSSION

We analyze the molecular mechanisms for the O–H bend overtone and O–H bend fundamental relaxation in liquid water. The Fourier transform of the autocorrelation function of the force acting on the O–H bend overtone in both rigid (Fig.1(a)) and flexible solvents (Fig.1(b)), is shown in Fig.1. It is obtained by using the Wiener-Khintchine theorem with a Hanning window [50]. For rigid solvent (Fig.1(a)), there is a broad peak at the region less than 1000 cm<sup>-1</sup>, which comes from the low-frequency libration and rotations of all molecules [41]. For the O–H bend overtone relaxation, there are two possible pathways: one is transition to the

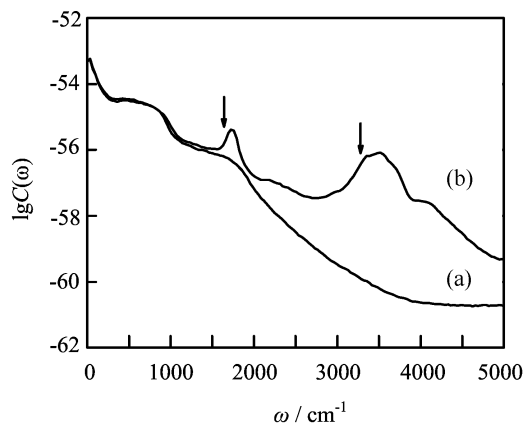


FIG. 1 Fourier transforms of the force TCF of O–H bend overtone of H<sub>2</sub>O in both rigid (a) and flexible (b) H<sub>2</sub>O. Arrows indicate the transition frequencies from the O–H bend overtone to bend fundamental and to ground state of H<sub>2</sub>O.

TABLE II Transition rate constants from the O–H bend overtone (020) to final state  $f$  in rigid H<sub>2</sub>O

| Final state $f$        | $\omega_f/\text{cm}^{-1}$ | $k_{if}/\text{s}^{-1}$     |
|------------------------|---------------------------|----------------------------|
| Bend fundamental (010) | 1640                      | $1.1492989 \times 10^{13}$ |
| Ground state (000)     | 3280                      | $5.9588865 \times 10^7$    |

O–H bend fundamental, the other is transition to the ground state. The relaxation rate constants of these two cases calculated from Eq.(7) as well as the transition frequencies of O–H bend overtone in rigid solvent are listed in Table II. The levels ( $ijk$ ) are labeled according to the standard ordering (O–H symmetric stretch, bend, and O–H asymmetric stretch). It is seen from Table II that the main relaxation pathway of O–H bend overtone (020) is the transition to the bend fundamental (010), which agrees well with the mechanisms proposed by Dlott [29] and Elsaesser [34]. The calculated total relaxation time  $T_1$  for O–H bend overtone is 174 fs. The total relaxation time  $T_1$  is determined by  $1/T = \sum_{i \neq f} k_{if}$ .

For the flexible solvent, with one exception, there is a significant increase in the magnitude of the spectral density at the frequency  $1730 \text{ cm}^{-1}$  due to the bend band of neat water, and at  $3450 \text{ cm}^{-1}$  due to the stretch vibrational band of neat water. The exception is one broad peak appearing below  $1000 \text{ cm}^{-1}$  which is the same as that in the rigid solvent. This peak comes from the low-frequency libration and rotations of all molecules [41]. For the transition from O–H bend overtone (020) to the bend fundamental (010) at  $1640 \text{ cm}^{-1}$ , the flexible spectral density is greater than the rigid one, which corresponds to the creation of one quantum solvent bend ( $\omega_s = 1730 \text{ cm}^{-1}$ ) and depletion of several quanta of translations and rotations. A significant increase in the spectral density with the flexible solvents

is observed for a transition to the ground state (000) at  $3280 \text{ cm}^{-1}$ . There are two possible mechanisms for this transition. One involves the creation of two quanta of the solvent bend ( $\omega_s = 1730 \text{ cm}^{-1}$ ) and absorption of several quanta of low-frequency translations and rotations (Case 1), and the other involves the creation of one quantum of the solvent stretch ( $\omega_s = 3450 \text{ cm}^{-1}$ ) and the depletion of several quanta of low frequency translations and rotations (Case 2).

Table III lists the rate constants of O–H bend overtone relaxation in the flexible H<sub>2</sub>O obtained from Eq.(7). For the transition to the ground state (000) at  $3280 \text{ cm}^{-1}$ , the relaxation rate of Case 1 ( $3.923638 \times 10^{10}$ ) is four times larger than the Case 2, which is  $9.715281 \times 10^9$ . Therefore, the mechanism for this transition is the excitation of two quanta of solvent bend, minus assorted translations and rotations. From Table III, we find that the primary relaxation channel of O–H bend overtone is dominated by the transition to the O–H bend fundamental, which agrees well with the mechanisms proposed by Dlott [29] and Elsaesser [34]. There is also a significant contribution from transition to the ground state. The calculated total relaxation time  $T_1$  for O–H bend overtone is 115 fs.

The relaxation rate constants of the O–H bend fundamental of H<sub>2</sub>O in both rigid and flexible solvents are listed in Table IV. The relaxation time  $T_1$  of O–H bend fundamental in rigid solvents is 499 fs. The relaxation is accelerated through the resonant energy transfer to the solvent bend vibration when solvent vibrations are included and calculated relaxation time is 204 fs, which agrees well with the experimental results obtained by Lindner [35] and Elsaesser [34].

In summary, the relaxation of the O–H bend overtone for water molecule in liquid water involves the following sequence of steps: A transition to O–H bend fundamental with excitation of one quantum of solvent bend, then the O–H bend fundamental relaxes to the ground state. This result agrees well with the recent experimental observation reported by Elsaesser [34].

#### IV. CONCLUSION

We have studied the vibrational energy relaxation of the O–H bend overtone and O–H bend fundamental in both rigid and flexible solvent H<sub>2</sub>O at 300 K, using Landau-Teller theory and molecular dynamics simulation. The calculated relaxation time for the O–H bend overtone is 174 fs for the rigid solvent and it decreases to 115 ps when solvent vibrations are included. The main pathway of the O–H bend overtone relaxation is a transition to the bend fundamental for both rigid and flexible solvent, which agrees well with the proposed mechanisms by experimental groups. The main pathway of O–H bend fundamental is transition to the ground state through the resonant energy transfer to the solvent bend vibration with a relaxation time of

TABLE III Transition rate constants from the O–H bend overtone (020) to final state  $f$  in flexible H<sub>2</sub>O

| Final state $f$             | $\omega_{if}/\text{cm}^{-1}$ | $k_{if}/\text{s}^{-1}$     | Channel  |
|-----------------------------|------------------------------|----------------------------|--|
| Bend fundamental (010)      | 1640                         | $1.7350173 \times 10^{13}$ | Via one quantum solvent bend, minus assorted translations and rotations    |
| Ground state (000) (Case 1) | 3280                         | $3.9236380 \times 10^{10}$ | Via two quanta of solvent bend, minus assorted translations and rotations  |
| Ground state (000) (Case 2) | 3280                         | $9.7152812 \times 10^9$    | Via one quantum solvent stretch, minus assorted translations and rotations |

TABLE IV Transition rate constants from the O–H bend fundamental (010) to final state  $f$  in both rigid and flexible H<sub>2</sub>O

| Final state $f$                 | $\omega_{if}/\text{cm}^{-1}$ | $k_{if}/\text{s}^{-1}$     | Channel   |
|---------------------------------|------------------------------|----------------------------|---|
| Ground state (rigid solvent)    | 1640                         | $2.0042520 \times 10^{12}$ | –   |
| Ground state (flexible solvent) | 1640                         | $4.9009201 \times 10^{12}$ | Via one quantum solvent bend, minus assorted translations and rotations |

204 fs, which agrees well with the experiment results.

## V. ACKNOWLEDGMENTS

The author is very grateful to Professor Jiu-shu Shao for his assistance and helpful discussion and critical reading the manuscript. I also would like to thank Dr. C. P. Lawrence, Prof. Jian-min Tao, Mr. Yun Zhou and Mrs. Lan Liu for their kind help. This work was supported by the National Natural Science Foundation of China (No.20225310 and No.20533060) and the Chinese Academy of Sciences.

- [1] M. D. Fayer, *Ultrafast Infrared and Raman Spectroscopy*, New York: Marcel Dekker, (2001).
- [2] R. Rey, K. B. Miller, and J. T. Hynes, *Chem. Rev.* **104**, 1915 (2004).
- [3] E. T. J. Nibbering and T. Elsaesser, *Chem. Rev.* **104**, 1887 (2004).
- [4] J. T. Fourkas, *Liquid Dynamics: Experiment, Simulation, and Theory*, Washington, DC: American Chemical Society, (2002).
- [5] N. Nandi, K. Bhattacharyya, and B. Bagchi, *Chem. Rev.* **100**, 2013 (2000).
- [6] S. K. Pal, J. Peon, B. Bagchi, and A. H. Zewail, *J. Phys. Chem. B* **106**, 12376 (2002).
- [7] T. Elsaesser, *Ultrafast Hydrogen Bonding Dynamics and Proton Transfer Processes in the Condensed Phase*, Dordrecht: Kluwer Academic Publishers, (2002).
- [8] J. Chesnoy and G. M. Gale, *Ann. Phys. Paris* **9**, 893 (1984).
- [9] D. W. Oxtoby, *Annu. Rev. Phys. Chem.* **32**, 77 (1981).
- [10] J. C. Owrutsky, D. Raftery, and R. M. Hochstrasser, *Annu. Rev. Phys. Chem.* **45**, 519 (1994).
- [11] D. W. Oxtoby, *Adv. Chem. Phys.* **47**, 487 (1981).
- [12] S. Okazaki, *Adv. Chem. Phys.* **118**, 191 (2001), and references therein.
- [13] T. Terashima, M. Shiga, and S. Okazaki, *J. Chem. Phys.* **114**, 5663 (2001).
- [14] Y. Deng, B. M. Ladanyi, and R. M. Stratt, *J. Chem. Phys.* **117**, 10752 (2002).
- [15] J. A. Poulsen and P. J. Rossky, *J. Chem. Phys.* **115**, 8014 (2001).
- [16] R. M. Whitnell, K. R. Wilson, and J. T. Hynes, *J. Chem. Phys.* **96**, 5354 (1992).
- [17] R. Rey and J. T. Hynes, *J. Chem. Phys.* **104**, 2356 (1996).
- [18] C. P. Lawrence and J. L. Skinner, *J. Chem. Phys.* **117**, 5827 (2002).
- [19] C. P. Lawrence and J. L. Skinner, *J. Chem. Phys.* **119**, 1623 (2003).
- [20] R. Rey and J. T. Hynes, *J. Chem. Phys.* **108**, 142 (1998).
- [21] A. Morita and S. Kato, *J. Chem. Phys.* **109**, 5511 (1998).
- [22] T. S. Gulmen and E. L. Sibert III, *J. Phys. Chem. A* **108**, 2389 (2004).
- [23] A. J. Lock, S. Woutersen, and H. J. Bakker, *J. Phys. Chem. A* **105**, 1238 (2001).
- [24] A. J. Lock and H. J. Bakker, *J. Chem. Phys.* **117**, 1708 (2002).
- [25] D. D. Dlott, *Chem. Phys.* **266**, 149 (2001), and references therein.
- [26] A. Pakoulev, Z. Wang, and D. D. Dlott, *Chem. Phys. Lett.* **371**, 594 (2003).
- [27] J. B. Asbury, T. Steinel, C. Stromberg, S. A. Corcelli, C. P. Lawrence, J. L. Skinner, and M. D. Fayer, *J. Phys. Chem. A* **108**, 1107 (2004).
- [28] G. C. Tian, *Chem. Phys.* **328**, 216 (2006).
- [29] J. C. Dequak, S. T. Rhea, L. K. Iwaki, and D. D. Dlott, *J. Phys. Chem. A* **104**, 4866 (2000).
- [30] Z. Wang, A. Pakoulev, and D. D. Dlott, *Chem. Phys. Lett.* **378**, 281 (2003).
- [31] A. Pakoulev, Z. Wang, Y. Pang, and D. D. Dlott, *Chem. Phys. Lett.* **380**, 404 (2003).
- [32] M. L. Cowan, B. D. Bruner, N. Huse, J. R. Dwyer, B. Chugh, E. T. J. Nibbering, T. Elsaesser, and R. J. D. Miller, *Nature* **434**, 199 (2005).
- [33] N. Huse, S. Ashihara, E. T. J. Nibbering, and T. El-

- saesser, Chem. Phys. Lett. **404**, 389 (2005).
- [34] S. Ashihara, N. Huse, E. T. J. Nibbering, and T. Elsaesser, Chem. Phys. Lett. **424**, 66 (2006).
- [35] J. Lindner, P. Vöhringer, M. S. Pshonichnikov, D. Cringus, D. A. Wiersna, and M. Mostovoy, Chem. Phys. Lett. **421**, 329 (2006).
- [36] R. A. Larsen and S. Woutersen, J. Chem. Phys. **121**, 12143 (2004).
- [37] M. G. Sceats and S. A. Rice, J. Chem. Phys. **71**, 973 (1979).
- [38] H. J. C. Berendsen, J. R. Grigera, and T. P. Straatsma, J. Phys. Chem. **91**, 6269 (1987).
- [39] K. Toukan and A. Rahman, Phys. Rev. B **31**, 2643 (1985).
- [40] C. P. Lawrence and J. L. Skinner, Chem. Phys. Lett. **372**, 842 (2003).
- [41] J. Martí, J. A. Padró, and E. Guàrdia, Mol. Sim. **11**, 321 (1993).
- [42] W. H. Miller, J. Chem. Phys. **53**, 3578 (1970).
- [43] W. H. Miller, J. Phys. Chem. A **108**, 2942 (2001).
- [44] J. T. Yardley, *Introduction to Molecular Energy Transfer*, New York: Academic, (1980).
- [45] S. A. Egorov and J. L. Skinner, Chem. Phys. Lett. **293**, 469 (1999).
- [46] S. A. Egorov, K. F. Everitt, and J. L. Skinner, J. Phys. Chem. A **103**, 9494 (1999).
- [47] J. L. Skinner and K. Park, J. Phys. Chem. B **105**, 6716 (2001).
- [48] W. Smith and T. Forester, J. Mol. Graphics **14**, 136 (1996).
- [49] M. P. Allen and D. J. Tildesley, *Computer Simulation of Liquids*, Oxford: Clarendon, (1987).
- [50] W. H. Press, B. P. Flannory, S. A. Teukolsky, and W. T. Vetterling, *Numerical Recipes*, Cambridge: Cambridge University Press, (1986).